PLOS | GENETICS

RESEARCH ARTICLE

Integration Analysis of Three *Omics* Data Using Penalized Regression Methods: An Application to Bladder Cancer

Silvia Pineda[1,2], Francisco X. Real[3,4], Manolis Kogevinas[5], Alfredo Carrato[6], Stephen J. Chanock[7], Núria Malats[1☯*], Kristel Van Steen[2,8☯*]

1 Genetic and Molecular Epidemiology Group, Spanish National Cancer Research Centre (CNIO), Madrid, Spain, **2** Systems and Modeling Unit–BIO3, Montefiore Institute, Liège, Belgium, **3** Epithelial Carcinogenesis Group, Spanish National Cancer Research Centre (CNIO), Madrid, Spain, **4** Departament de Ciències Experimentals i de la Salut, Universitat Pompeu Fabra, Barcelona, Spain, **5** Centre for Research in Environmental Epidemiology (CREAL) and Parc de Salut Mar, Barcelona, Spain, **6** Servicio de Oncología, Hospital Universitario Ramon y Cajal, Madrid, and Servicio de Oncología, Hospital Universitario de Elche, Alicante, Spain, **7** Division of Cancer Epidemiology and Genetics, National Cancer Institute, Department of Health and Human Services, Bethesda, Maryland, United States of America, **8** Systems Biology and Chemical Biology, GIGA-R, Liège, Belgium

☯ These authors contributed equally to this work.
* nmalats@cnio.es (NM); kristel.vansteen@ulg.ac.be (KVS)

Abstract

Omics data integration is becoming necessary to investigate the genomic mechanisms involved in complex diseases. During the integration process, many challenges arise such as data heterogeneity, the smaller number of individuals in comparison to the number of parameters, multicollinearity, and interpretation and validation of results due to their complexity and lack of knowledge about biological processes. To overcome some of these issues, innovative statistical approaches are being developed. In this work, we propose a permutation-based method to concomitantly assess significance and correct by multiple testing with the MaxT algorithm. This was applied with penalized regression methods (LASSO and ENET) when exploring relationships between common genetic variants, DNA methylation and gene expression measured in bladder tumor samples. The overall analysis flow consisted of three steps: (1) SNPs/CpGs were selected per each gene probe within 1Mb window upstream and downstream the gene; (2) LASSO and ENET were applied to assess the association between each expression probe and the selected SNPs/CpGs in three multivariable models (SNP, CPG, and Global models, the latter integrating SNPs and CPGs); and (3) the significance of each model was assessed using the permutation-based MaxT method. We identified 48 genes whose expression levels were significantly associated with both SNPs and CPGs. Importantly, 36 (75%) of them were replicated in an independent data set (TCGA) and the performance of the proposed method was checked with a simulation study. We further support our results with a biological interpretation based on an enrichment analysis. The approach we propose allows reducing computational time and is flexible and easy to implement when analyzing several types of *omics* data. Our results highlight the importance of integrating *omics* data by applying appropriate statistical

OPEN ACCESS

Citation: Pineda S, Real FX, Kogevinas M, Carrato A, Chanock SJ, Malats N, et al. (2015) Integration Analysis of Three *Omics* Data Using Penalized Regression Methods: An Application to Bladder Cancer. PLoS Genet 11(12): e1005689. doi:10.1371/journal.pgen.1005689

Editor: David McConkey, The University of Texas M. D. Anderson Cancer Center, UNITED STATES

Received: June 8, 2015

Accepted: October 30, 2015

Published: December 8, 2015

Data Availability Statement: Common genetic variation (GSE51641), DNA methylation (GSE71666), and gene expression (GSE71576) data for the discovery phase are available in GEO.

Funding: The work was partially supported by Fondo de Investigaciones Sanitarias (FIS), Instituto de Salud Carlos III, Spain (#PI06-1614 and #PI12-00815); Red Temática de Investigación Cooperativa en Cáncer, Spain (#RD12/0036/0034 and #RD12/0036/0050); EU-FP7-HEALTH (F2-2008-201663-UROMOL and F2-2008-201333-DECanBio); USA-NIH (RO1-CA089715 and NO2-CP-11015); and European

Cooperation in Science and Technology (COST Action #BM1204: EU_Pancreas). SP was funded by a Obra Social Fundación "la Caixa". The funders had no role in study design, data collection and analysis, decision to publish, or preparation of the manuscript.

Competing Interests: The authors have declared that no competing interests exist.

strategies to discover new insights into the complex genetic mechanisms involved in disease conditions.

Author Summary

At present, it is already possible to generate different type of *omics*–high throughput–data in the same individuals. However, we lack methodology to adequately combine them. Many challenges arise while the amount of data increases and we need to find the way to identify and understand the complex relationships when integrating data. In this regard, new statistical approaches are needed, such as the ones we propose and apply here to integrate three types of *omics* data (genomics, epigenomics, and transcriptomics) generated using bladder cancer tumor samples. These innovative approaches (LASSO and ENET combined with a permutation-based MaxT method) allowed us to find 48 genes whose expression levels were significantly associated with genomics and epigenomics markers. The adequacy of this approach was confirmed by the use of an independent data set from The Cancer Genome Atlas Consortium: 75% of the genes were replicated. Previous sound biological evidences further support the results obtained.

Introduction

Integrating different *omics* data types, such as genomics, epigenomics and transcriptomics, may provide a new strategy to discover unknown genomic mechanisms involved in complex diseases [1–3]. In cancer, tumor initiation and progression are the consequence of alterations in multiple pathways and biological processes including gene mutations, epigenetic changes, modifications in gene regulation, and environmental influences. In the process to integrate all of this information many challenges arise, among them the high dimensionality of data—since >2 *omics* data sets with millions of measurements are available from the same set of individuals—and the huge heterogeneity of *omics* data due to the different measurement scales [4]. Besides that, the data might be highly correlated, i.e. Single Nucleotide Polymorphisms (SNPs) that are in high linkage disequilibrium (LD) block or DNA CpG sites that belong to the same CpG island, contributing to multicollinearity in the analysis. Another challenge in *omics* data integration regards to the very small number of individuals in comparison to the number of parameters ("n << p"). In addition, interpretation and validation of *omics* derived results require of resources that are still lacking at present. In this rapidly evolving scenario, advanced methodological techniques are continuously emerging, demanding the development of improved data analysis tools [5–7].

Integrative *omics* analysis refers to the combination of at least two different types of *omics* data. Relationships between two sets of *omics* parameters such as the expression quantitative trait loci (eQTL) [2,8,9] or the methylation-QTL (methQTL) [3,10,11], have been recently reported. The approach most commonly used for this type of pairwise analysis has been univariate models (i.e., Spearman/Pearson correlation or linear regression models), assuming that the changes in gene expression levels are only affected by one parameter. Until present, the combination of >2 *omics* data has been less explored.

Towards this end, the previously mentioned challenges are magnified and there is a lack of advanced methodologies to deal with them. Recently, we published an integrative framework as a first approach to integrate genomics, epigenomics, and transcriptomics in individuals with urothelial bladder cancer (UBC) [12]. In that work, we found that some gene expressions were co-regulated by both DNA methylation and genetic variants, both acting together in trans relationships. Therefore, the integration of multiple types of *omics* data by applying multivariable approaches becomes essential to understand the intricacy of the genomic mechanisms behind complex diseases and to overcome the abovementioned challenges.

In this regard, previous developments are Principal Component Analysis (PCA), to reduce data dimensionality, or Canonical Correlation Analysis (CCA) to investigate the overall correlation between two sets of variables. However, these methods are descriptive or exploratory techniques rather than hypothesis-testing tools. While some statistical applications have been developed in an *omics* integrative framework (sparse canonical correlation analysis [13], multiple factor analysis [14], or multivariate partial least square regression [15]), none of them offers the possibility to combine >2 *omics* data together in the same model.

The Least Absolute Shrinkage and Selection Operator (LASSO) proposed by Tibshirani in 1996 [16] and the Elastic Net (ENET) proposed by Hui Zou and Trevor Hastie in 2005 [17] are penalized regression methods that, after appropriate standardization, can model more than one type of *omics* data, face multicollinearity issues, and mitigate the "n << p" problem. More importantly, both methods simultaneously execute variable selection and parameter estimation, thus reducing the computation time, while the traditional methods work on the two problems separately, first selecting the relevant parameters and then computing the estimates. LASSO and ENET have already been applied to GWAS studies [18–20] as well as in the context of integrative studies [21]. One limitation of penalized regression techniques is that the penalty produces biased estimators; consequently, standard errors are not meaningful and cannot provide p-values to assess significance. Here, we propose a permutation-based approach to assess significance and we combine it with a correction for Multiple Testing (MT) using the MaxT algorithm [22]. We apply this permutation-based MaxT method with LASSO and ENET to identify relationships between common genetic variation, DNA methylation, and gene expression, all determined in UBC tumor samples. Specifically, we first built a two *omics* integrative model associating SNPs or CpGs with gene expression levels and, then, we integrated the three *omics* data to assess whether changes in gene expression levels could be confounded/modified by genetic variants and/or DNA methylation.

Material and Methods

Penalized regression methods

LASSO and ENET penalized regression methods are applied to high-dimensional problems with a large number of parameters. The penalization produces a shrinkage of the regression coefficients towards zero given a sparse model reducing the irrelevant parameters. Both methods deal with highly correlated variables though in a different way. LASSO tends to select one variable from a group of correlated features whereas ENET selects the whole group of variables, when evidence for their relevance exists. The shrunk estimators introduce a bias while reducing the variance resulting in a better precision and accuracy model and, therefore, increasing its statistical power.

Definition of the methods. Consider the standard linear regression model where $y = (y_1, \ldots y_n)^t$ is the response variable and $x = (x_{1j}, \ldots x_{nj})^t$ $j = 1, \ldots p$ are the standardized predictors, the LASSO solves the l_1 penalized regression problem, the Ridge regression [23] solves the l_2 penalized regression problem and the ENET is the combination between the l_1 and l_2 penalized regression problem.

For the LASSO and ENET estimates $\widehat{\beta_0}, \widehat{\beta} = (\widehat{\beta}_1, \ldots, \widehat{\beta}_p)^t$; $(\widehat{\beta_0}, \widehat{\beta})$ are defined by

$$(\widehat{\beta_0}, \widehat{\beta}) = \arg min \left\{ \sum_{i=1}^{n} \left(y_i - \beta_0 - \sum_{j=1}^{p} \beta_j x_{ij} \right)^2 \right\}$$

with the restrictions:

$$\sum_{j=1}^{p} |\beta_j| \leq t \; (LASSO), \tag{1}$$

$$\sum_{j=1}^{p} |\beta_j| \leq t \,, \sum_{j=1}^{p} \beta_j^2 \leq t \;\; (ENET). \tag{2}$$

Here, $t \geq 0$ is the tuning parameter that controls the amount of shrinkage that is applied to the estimates. For $\widehat{\beta}_j^0$ the un-penalized least squares estimate, $t_0 = \sum |\widehat{\beta}_j^0|$. Values of $t < t_0$ will lead to shrinkage towards 0; some coefficients may be exactly equal to 0.

Using the Lagrangian form, this optimization problem is equivalent to (LASSO):

$$\widehat{\beta}_{lasso} = argmin \left\{ \frac{1}{N} \sum_{i=1}^{N} (y_i - x_i \beta)^2 + \lambda \sum_{j=1}^{p} |\beta_j| \right\} \tag{3}$$

where λ is the penalty parameter related to t. To obtain the optimal penalty, k-fold cross validation (CV) was applied [24] maximizing the penalized log-likelihood function.

(ENET):

$$\widehat{\beta}_{enet} = argmin \left\{ \frac{1}{N} \sum_{i=1}^{N} (y_i - x_i \beta)^2 + \lambda_1 \sum_{j=1}^{p} |\beta_j| + \lambda_2 \sum_{j=1}^{p} \beta_j^2 \right\}, \tag{4}$$

where λ_1, λ_2 are the penalty parameters related to t. In this sense, ENET can be viewed as a penalized least squares method. With $\alpha = \lambda_2/(\lambda_1 + \lambda_2)$, solving $\widehat{\beta}_{enet}$ in Eq (4) is equivalent to the following optimization problem:

$$\widehat{\beta}_{enet} = argmin \left\{ \frac{1}{N} \sum_{i=1}^{N} (y_i - x_i \beta)^2 + (1 - \alpha) \sum_{j=1}^{p} |\beta_j| + \alpha \sum_{j=1}^{p} \beta_j^2 \right\} \tag{5}$$

This expression involves a convex combination of the LASSO and ridge penalty. When $\alpha =$ 1 the ENET becomes ridge regression and when α =0 the ENET becomes LASSO. To obtain the optimal penalty (λ), k-fold CV selecting the best α was applied. This value was obtained using a vector of $\alpha \epsilon (0.01, 0.99)$ *by* 0.01.

The LASSO and ENET methods described above were applied to our data with the R package glmnet, that relies on cyclical coordinate descent, computed along a regularization path [25]. To avoid small sample size limitations in variable selection while not introducing an important bias k = 5 was used in the k-fold CV.

These methods are promising in the context of high-throughput data but one of their drawbacks is that they do not provide p-values to assess statistical significance of relationships, nor give a formal assessment of the overall goodness-of-fit. Therefore, a permutation based strategy was adopted to assess significance of discovered relationships combined with a MT correction approach (MaxT algorithm [22]) building upon the statistical concept of deviance. The deviance is used to compare two models and in this case we defined it as

$$Deviance = 2[loglik(full_{model}) - loglik(null_{model})].$$

Here *loglik* is the loglikelihood function, $full_{model}$ refers to the model with the parameters selected by LASSO or ENET, and $null_{model}$ is the model with only the intercept estimated. Thus, the interpretation would be, the higher the deviance the better the model.

Permutation-based MaxT method

MaxT algorithm of Westfall & Young [22] is a step-down FWER-controlling MT procedure. The method uses the raw p-values or directly the statistics as explained in [26]. Using this approach, the permutation needed to obtain the p-values was combined with the one needed to apply the MaxT algorithm saving computational time. In this work, we used the deviance obtained per each of the permuted LASSO/ENET model to compute the MaxT algorithm and individuals within gene expression measure were permuted, that is the dependent variable in the models. The algorithm is explained in Box 1.

Box 1. Permutation-based MaxT method

From the original data, order the deviance obtained per each observed statistics:

$$|D_{s1}| \geq |D_{s2}| \geq |D_{s3}| \geq \cdots \geq |D_{sm}|.$$

For the bth permutation, b = 1. . .B

1. Permute the n individuals of each of the vectors $Y_m = (y_1, \ldots y_n)_m$
2. Compute the statistics $D_{1b,\ldots}D_{mb}$
3. Compute the $U_{i,b} = \max_{l = i\ldots m}|D_{sl,b}|$, the successive step-down procedure is: $U_{m,b} = |D_{sm,b}|$

. . .

$$U_{2,b} = \max|D_{s2,b}, D_{s3,b}, \ldots, D_{sm,b}|$$

$$U_{1,b} = \max|D_{s1,b}, D_{s2,b}, D_{s3,b}, \ldots, D_{sm,b}|$$

4. The steps are repeated B times and the adjusted p-values are estimated by:

$$P_{adj,i} = \frac{\#\{b; U_{ib} \geq |D_{si}|\}}{B} \; for\; i = 1 \ldots m$$

Discovery phase: The Spanish Bladder Cancer/EPICURO Study

70 patients with a histologically confirmed UBC were recruited in 2 hospitals during 1997–1998 as part of the pilot phase of the Spanish Bladder Cancer/EPICURO Study. According to established criteria based on tumor stage and grade for UBC, the tumors were classified as low-grade non-muscle invasive, high-grade non-muscle invasive, and muscle invasive. Three sets of

omics data were obtained using fresh tumor tissue, including common genetic variation (GSE51641), DNA methylation (GSE71666), and gene expression (GSE71576). The three *omics* data overlapped in 27 individuals that are included in this study and comprise 44% low-grade non-muscle invasive tumors, 30% high-grade non-muscle invasive tumors and 26% muscle invasive tumors. S1 Table shows the IDs of the 27 samples used in the following analysis. The local ethics committee of the participating centers approved the study and written informed consent was obtained from all participants at the time of recruitment.

Genotyping of tumor samples was performed using Illumina HumanHap 1M array. A total of 1,047,101 SNPs were determined in 46 individuals and, after the standard quality control and filter the SNPs that were in perfect LD ($r^2 = 1$), they resulted in 567,513 SNPs. The application of multivariable models required no missing values, so genotypes were imputed with BEAGLE 3.0 method [27]. CpG methylation data was generated using the Infinium Human Methylation 27 BeadChip Kit. At each CpG site, the methylation levels were measured with M-values using the log2 transformation of the β-values since they are more statistically valid due to a better approximation of the homoscedasticity. The initial number of CpGs in the studied array was 27,578 and after background normalization and QC, a total number of 23,034 CpGs were left for analysis. Gene expression data were obtained from 44 tumor samples using the Affymetrix DNA Microarray Human Gene 1.0 ST Array with 32,321 probes. After the application of QC, it resulted in 20,899 probes determined in 37 individuals. Further details about the preprocessing of the data and the quality control applied can be found elsewhere [12]. The three measures were annotated using the UCSC hg19, NCBI build 37 to make them comparable and homogenize their position in the genome.

Simulation study

To generate a simulation sample, the association between SNPs and/or CpGs with gene expression was broken and therefore no significant results should be observed. To do that, 10-gene expression probes were randomly selected from our discovery sample showing no correlation structure between the probes and following a multivariate normal distribution. Then, the mean ($\mu = 8.4$) and variance ($\sigma^2 = 0.4$) of all the probes together were obtained. Finally, a simulated set of gene expression probes was generated using the normal distribution obtained and considering the same sample size of the discovery phase ($p = 20{,}899$ probes and $N = 27$ individuals).

Replication phase: The Cancer Genome Atlas (TCGA)

UBC tumor data were obtained from The Cancer Genome Atlas (TCGA) consortium (https://tcga-data.nci.nih.gov/tcga/) to replicate our findings. Data was downloaded and processed with the TCGA-Assembler [28]. The study included only individuals with muscle invasive UBC and the tumors were profiled with genome wide 6.0 Affymetrix, RNASeqV2, and HumanMethylation450K Illumina arrays yielding data for 20,502 gene expression probes, 905,422 SNPs, and 350,271 CpGs. The total number of individuals with overlapping data from the three platforms was 238 and they were used in the replication phase of this contribution. S2 Table shows the IDs corresponding to these 238 samples.

Overall analysis flow

Penalized regression methods LASSO and ENET were applied to the discovery data in combination with the proposed permutation-based MaxT method to select the SNPs and/or CpGs associated with gene expression levels in the following multivariable models:

SNP model:

$$Gene\ Expression\ levels_i = \alpha_1 SNP_1 + \alpha_2 SNP_2 + \cdots + \alpha_p SNP_p;\ i = 1 \ldots m$$

CPG model:

$$Gene\ Expression\ levels_i = \gamma_1 CPG_1 + \gamma_2 CPG_2 + \cdots + \gamma_p CPG_p;\ i = 1 \ldots m$$

Global model = SNP + CPG model:

$$Gene\ Expression\ levels_i = \alpha_1 SNP_1 + \cdots + \alpha_p SNP_p + \gamma_1 CPG_1 + \cdots + \gamma_p CPG_p;\ i = 1 \ldots m$$

To apply this integrative idea to our set of data the following steps were performed: (1) SNPs and CpGs that were in a 1MB window upstream and downstream were selected from each probe in the gene expression array; (2) LASSO and ENET were applied to each probe and model (SNP, CpG, and Global models) obtaining the deviance per model; and (3), the permutation-based MaxT method was applied to obtain the adjusted p-values (B = 100 permutations and significant adjusted p-value < 0.1). The scenario and workflow is represented in Fig 1.

Subsequently, this analysis flow was applied to the simulated data set using the same criteria. In the replication scenario, we aimed at determining whether the genes that were significant in the discovery phase were also significant in the replication dataset. Therefore, the analysis was restricted to the genes found to be significant in the discovery phase considering all models (SNP, CPG and/or Global) and methods (LASSO and/or ENET). Following the pipeline shown in Fig 1, we focused on the significant genes found in the discovery phase and SNPs and CpGs were selected in 1MB window from the TCGA database, even if the SNPs and CpGs were not the same as those analyzed in the discovery phase. Second, LASSO and/or ENET were conducted to SNP, CPG, and/or Global models. Finally, the permutation-based MaxT method was applied to obtain significance and correct for multiple testing. The replication analysis was performed with the same software and criteria as in the discovery analysis.

Gene enrichment analysis

To provide a biological interpretation to the results, the entire list of the significant genes identified in the discovery phase by both LASSO and ENET, and by the three models, was used to perform a gene enrichment analysis with the bioinformatics tool DAVID [29,30]. The functional annotation clustering analysis module offered by DAVID was used. The gene term annotation is based on 14 annotation categories (Gene Ontology (GO), Biological process, GO Molecular Function, GO Cellular Component, KEGG Pathways, BioCarta Pathways, Swiss-Prot Keywords, BBID Pathways, SMART Domains, NIH Genetics Association DB, UniProt Sequence Features, COG/KOG Ontology, NCBI OMIM, InterPro Domains, and PIR Super-Family Names) collected in the DAVID tool knowledgebase (https://david.ncifcrf.gov/knowledgebase/DAVID_knowledgebase.html). The method identifies related genes by measuring the similarity of their global annotation profiles. So, the "grouping term" is based on the idea that two genes that have similar annotation profiles are functionally related. Each group term provides an enrichment score (ES) that indicates biological significance when $\geq$1.3 (equivalent to non-log scale 0.05). DAVID also provides a p-value to examine the significance of gene-term enrichment, which is corrected by Benjamini MT [31].

Results

Discovery phase

LASSO and ENET were applied to 20,899 gene expression probes in each of the three models. Under the conditions mentioned above, LASSO yielded 9 genes with a significant signal in the

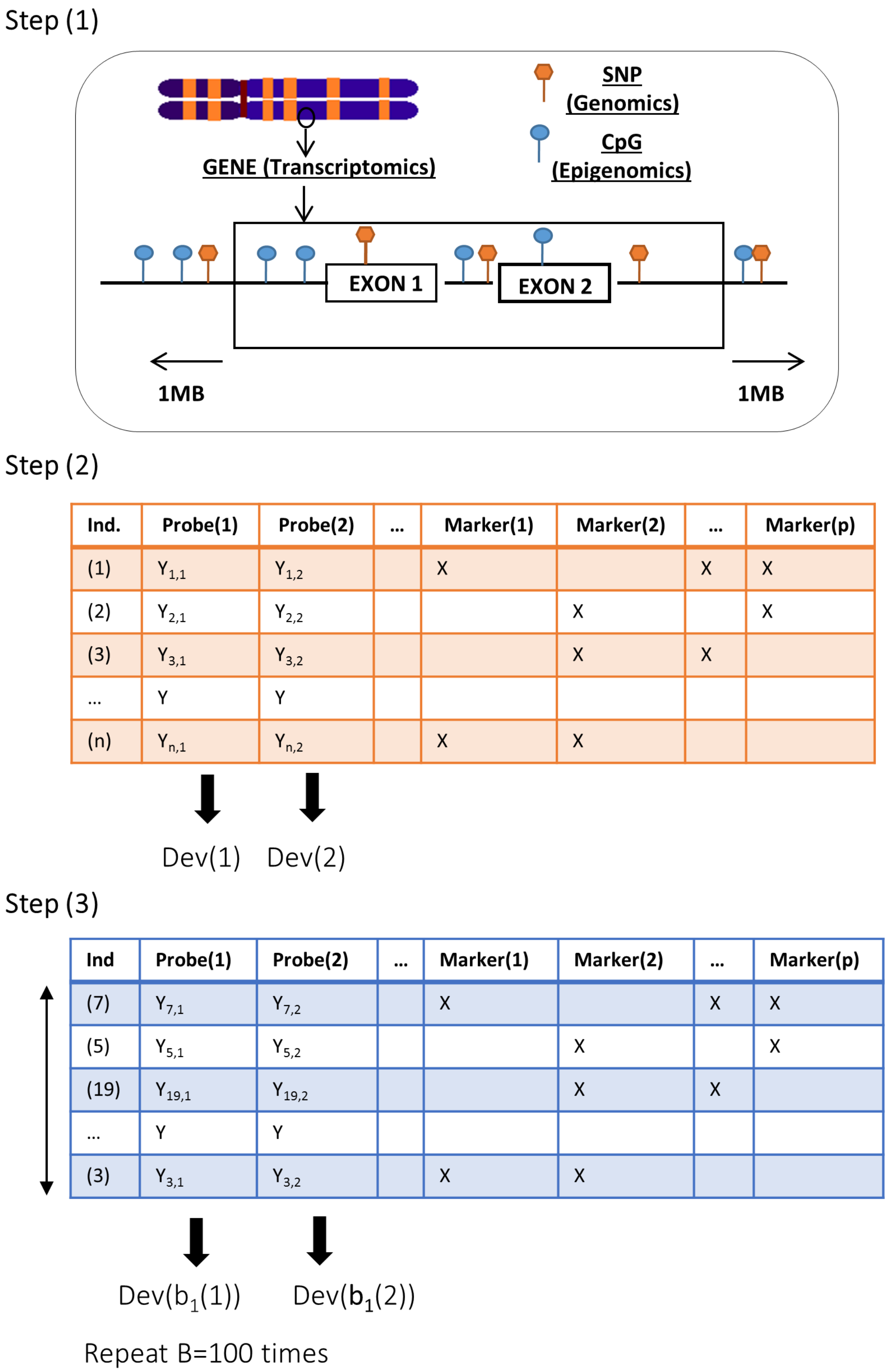

Ind.	Probe(1)	Probe(2)	…	Marker(1)	Marker(2)	…	Marker(p)
(1)	$Y_{1,1}$	$Y_{1,2}$		X		X	X
(2)	$Y_{2,1}$	$Y_{2,2}$			X		X
(3)	$Y_{3,1}$	$Y_{3,2}$			X	X	
…	Y	Y					
(n)	$Y_{n,1}$	$Y_{n,2}$		X	X		

Ind	Probe(1)	Probe(2)	…	Marker(1)	Marker(2)	…	Marker(p)
(7)	$Y_{7,1}$	$Y_{7,2}$		X		X	X
(5)	$Y_{5,1}$	$Y_{5,2}$			X		X
(19)	$Y_{19,1}$	$Y_{19,2}$			X	X	
…	Y	Y					
(3)	$Y_{3,1}$	$Y_{3,2}$		X	X		

Fig 1. Scenario and workflow of the overall analysis implemented. The integrative framework proposed is based on three steps. Step 1 corresponds to the selection of SNPs and CpGs in 1MB window upstream and downstream from each probe in the gene expression array. Step 2 corresponds to the application of LASSO and ENET to each probe obtaining the deviance per probe. Step 3 corresponds to the permutation-based MaxT method application where gene expression levels within the individuals are permuted B = 100 times obtaining the deviance per probe.

doi:10.1371/journal.pgen.1005689.g001

Table 1. Statistically significant genes associated with SNPs and/or CpGs selected by LASSO&Permuted based maxT algorithm.

Gene Name	Chromosome	Model	Deviance	p-value[1]
AIM2	1	SNPs	55.8	0.1
		CpGs	61.5	0.06
PLA2G2A	1	CpGs	71.4	0.01
S100A9	1	CpGs	53.7	0.03
		SNPs + CpGs	52.4	0.08
HMGCS2	1	CpGs	53.3	0.02
PIGR	1	CpGs	75.8	< 0.01
CTSE	1	CpGs	60.7	0.06
S100A2	1	SNPs + CpGs	58.7	0.04
CP	3	CpGs	51.1	0.02
TMEM45A	3	SNPs + CpGs	57.3	0.08
IGJ	4	CpGs	58.4	0.03
		SNPs + CpGs	59.0	0.09
UBD	6	SNPs + CpGs	75.0	0.07
TRIM31	6	SNPs + CpGs	47.1	0.1
PTN	7	SNPs	67.0	0.08
		SNPs + CpGs	92.0	< 0.01
ARHGEF35	7	SNPs + CpGs	49.6	0.09
CRH	8	SNPs + CpGs	56.7	0.1
CRTAC1	10	SNPs	66.2	0.03
MSMB	10	CpGs	67.3	0.06
CRTAC1	10	SNPs	60.9	0.1
		SNPs + CpGs		
TNNT3	11	CpGs	44.9	0.09
SAA1	11	SNPs + CpGs	127.8	0.04
SCCN1A	12	SNPs	57.9	0.08
		CpGs	58.8	0.03
KRT5	12	CpGs	58.2	0.03
TSPAN8	12	SNPs + CpGs	67.2	0.05
MYBPC1	12	SNPs + CpGs	74.5	0.08
SLC38A4	12	SNPs + CpGs	51.7	0.08
GTSF1	12	SNPs + CpGs	46.7	0.1
OLFM4	13	CpGs	60.0	0.06
FREM2	13	CpGs	46.0	0.06
		SNPs + CpGs	70.2	0.06
IGHD	14	SNPs + CpGs	59.4	0.1
C15orf48	15	CpGs	49.9	0.02
		SNPs + CpGs	83.7	0.05
CAPNS2	16	SNPs + CpGs	54.9	0.07
KRT20	17	CpGs	48.4	0.05
		SNPs + CpGs	93.7	< 0.01
KRT13	17	CpGs	53.6	0.02
SERPINB4	18	SNPs	98.4	< 0.01
		SNPs + CpGs	68.5	0.03
SERPINB3	18	SNPs	171.6	< 0.01
		SNPs + CpGs	162.7	< 0.01
CEACAM7	19	CpGs	76.0	< 0.01

(*Continued*)

Table 1. (*Continued*)

Gene Name	Chromosome	Model	Deviance	p-value[1]
CEACAM6	19	SNPs	79.6	0.01
CXCL17	19	SNPs + CpGs	46.8	0.1
CLIC6	21	SNPs	75.3	0.01
		CpGs	45.1	0.09
		SNPs + CpGs	75.3	0.07
GSTT1	22	SNPs	40.4	0.07

[1] The p-value was obtained after applying the permuted based–maxT algorithm and was therefore corrected for MT.

doi:10.1371/journal.pgen.1005689.t001

SNP model, 19 in the CpG model, and 23 in the Global model. Table 1 shows the significant genes, mapped to each probe, with its deviance and p-value. Fig 2A–2C display all the probes analyzed with their deviances represented across the genome. Detailed information about the SNPs and/or CpGs mapped to these genes is provided as Supplementary Material (S1–S6 Excel). ENET identified a lower number of significant genes: 11 in the SNP model, 6 in the CpG model, and 4 in the Global model. These results are shown in Table 2 and Fig 2D–2F. When the MT correction threshold was relaxed, ENET provided additional significant genes.

Some genes overlapped among methods and models: *CLIC6* was identified by the three LASSO models; *AIM2* and *SCNN1A* came out in the SNP and CpG models; *PTN*, *CRTAC1*, *SERPINB3* and *SERPINB4* were identified in the SNP and Global models; and *S100A9*, *IGJ*, *FREM2*, *C15orf48* and *KRT20* emerged in the CpG and Global models. Interestingly, 15 genes showed significance in the Global model when combining 3 *omics* data while they were not detected when analyzing only 2 types of *omics* data. The overlap of genes identified by the ENET model was lower: *MSMB* and *IGF2* were identified by the SNP and CpG models, and *PTN* and *SERPINB3* were selected by the SNP and the Global models. When comparing the methods, an overlap between LASSO and ENET was found for four (*PTN*, *SERPINB3*, *SERPINB4* and *CEACAM6*), one (*MSMB*), and three (*SERPINB3*, *PTN* and *IGHD*) significant genes in the SNP, CpG, and Global models, respectively. These results are displayed in Fig 3 using Venn diagrams. In the simulation study, as expected, no gene was significantly associated with any of the two methods and the three models. An example of the deviances of each gene for the SNP 303 model and LASSO method is shown in S1 Fig.

Replication phase

The replication study was restricted to those genes (n = 48) that showed significant results in the discovery phase and we applied the same models, methods, and criteria of analysis to the TCGA data. Overall, we were able to replicate 75% of the results: 36 out of the 48 genes yielded a significant association at least in one of the models considered. Regarding the LASSO models, we replicated 3/9 genes from the SNP models, 17/19 genes from the CPG models, and 19/23 genes from the Global models (Table 3). Regarding ENET, we replicated 3/10 genes from the SNP model, 3/6 genes from the CPG model, and 3/3 genes from the Global model (Table 4).

Gene enrichment analysis

Using DAVID, 46 out of 48 genes showing significant signals in the discovery phase were annotated from 14 public categories. After enrichment analysis, 7 clusters with an ES ≥1.3 were found (S3 Table). The cluster with the highest ES (3.5) regarded to the terms “extracellular region, secreted, and signal peptide” grouping the genes *OLFM4*, *CRTAC1*, *MSMB*, *IGJ*,

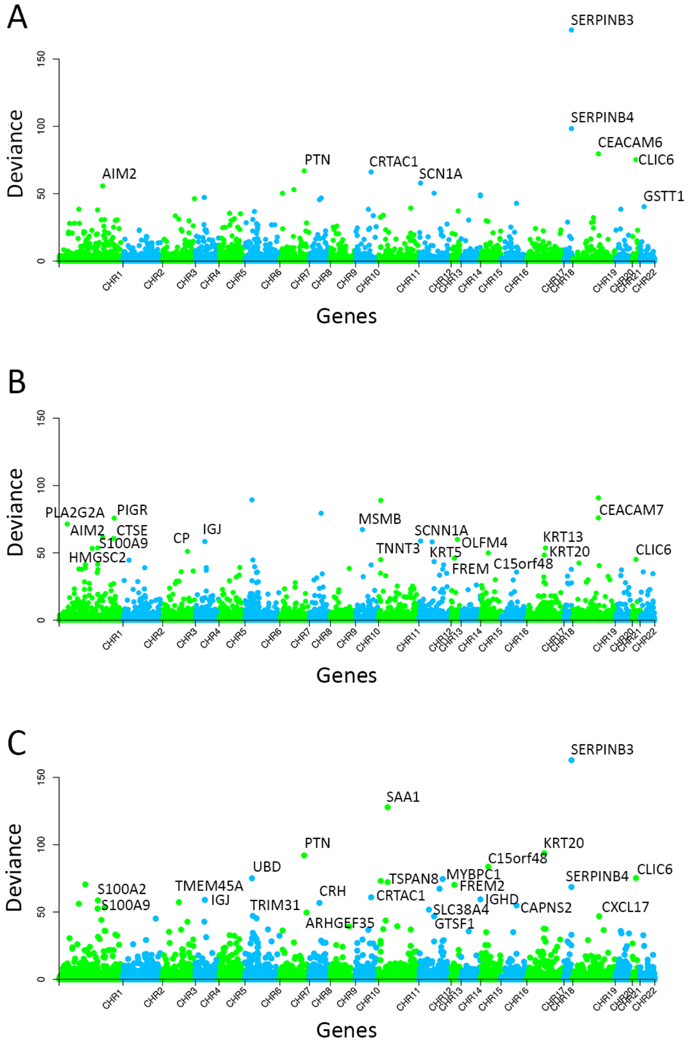

Fig 2. Deviance across the genome when applying LASSO and ENET to select SNPs, CpGs or both (Global model). The dots in the figure indicate the deviance of each gene located in the corresponding position in the genome. There are a total of 20,899 gene expression probes measured. Significant genes after applying the permutation-based MaxT method are tagged. The figures represent the deviance per gene expression probe using LASSO for the SNP model (A), the CpG model (B) and the Global model (C) and using ENET for the SNP model (D), the CpG model (E) and the Global model (F).

doi:10.1371/journal.pgen.1005689.g002

MMP7, *IGF2*, *PIGR*, *TCN1*, *CXCL17*, *S100A9*, *SAA1*, *IGHD*, *CRH*, *CTSE*, *FREM2*, *PLA2G2A*, *CEACAM7*, *CEACAM6*, *CEACAM5*, *REN*, *PTN*, *CP*.

The rest of the clusters with an ES ≥1.3 were not significant after MT correction. Cluster 5 (ES = 1.4) contains 3 genes coding for keratins (*KRT5*, *KRT13*, *KRT20*), cytoskeletal components that are regulated during urothelial differentiation, whose expression is altered in UBC, that have been proposed as markers for the molecular taxonomy of UBC [32]. In addition, cluster 7 "EF hand and calcium ion binding" (ES = 1.3) contains multiple genes shown to play an important role in cancer (*S100A9*, *S100A2*, *CAPNS2*, *ANXA10*, *CRTAC1*, *FREM2*, *MMP7*, *PLA2G2A*), including two members of the S100A family of proteins.

Discussion

Integration analysis is an emerging area in the field of *omics* data analysis to find new biological insights into complex traits [33]. In this regard, our pathophysiological understanding of

Table 2. Statistically significant genes associated with SNPs and/or CpGs selected by ENET&Permuted based maxT algorithm.

Gene Name	Chromosome	Model	Deviance	p-value[1]
REN	1	CPG	84.3	0.03
CRABP2	1	CPG	65.2	0.09
ANXA10	4	SNP	137.0	0.01
PTN	7	SNP	97.2	0.07
		SNP +CPG	102.5	0.09
MSMB	10	SNP	91.8	0.07
		CPG	78.9	0.06
MMP7	11	SNP	94.8	0.06
TCN1	11	SNP	88.9	0.07
IGF2	11	SNP	101.6	0.05
		CPG	92.1	0.04
MMP7	11	SNP + CPG	99.4	0.08
GTSF1	12	SNP	109.6	0.05
IGHD	14	SNP + CPG	97.5	0.1
SERPINB4	18	SNP	105.2	0.04
SERPINB3	18	SNP	171.6	0.02
		SNP + CPG	171.3	0.01
CEACAM6	19	SNP	108.4	0.03
NRLP2	19	CPG	84.2	0.04
CEACAM5	19	CPG	92.1	0.06
IGLJ3	22	SNP	97.7	0.05

[1] The p-value was obtained after applying the permuted based–maxT algorithm and corrected by MT.

doi:10.1371/journal.pgen.1005689.t002

cancer could be improved by using innovative approaches based on *omics* data to identify hidden mechanisms in which multiple factors are involved. We previously analyzed the set of *omics* data used here following a multi-stage approach by proposing an *omics* integration analysis framework. The results of this previous work highlighted relevant *omics* trans-acting relationships in UBC [12]. Here, we propose an *omics* integrative analysis pipeline using LASSO and ENET, and focus on cis-acting relationships that appear to have a predominant role in the regulation of gene expression [34]. The three *omics* data are combined in a large input matrix and then a permutationbased MaxT method is adapted to assess the significant models while correcting for MT.

In comparison with classical approaches [6,7], our strategy has several advantages, including the possibility of working with a large number of parameters, even if the sample size is small, dealing with more than one set of heterogeneous data with highly-correlated variables, and providing MT corrected p-values to assess the models' goodness of fit. Furthermore, the results are easily interpretable due to the dimensionality reduction during the variable selection process.

The expression of 48 genes was found to be significantly associated with SNPs and CpGs in UBC, pointing to new mechanisms in an intricate scenario where common genetic variants and DNA methylation regulate gene expression in cis-acting (1MB) relationships. Some of the genes were identified by the three models and by the two methods, likely underscoring the existence of true relationships.

The application of LASSO and ENET as part of the aforementioned integrative analysis framework led to different results. This is not surprising, mainly for two reasons: (1) the α

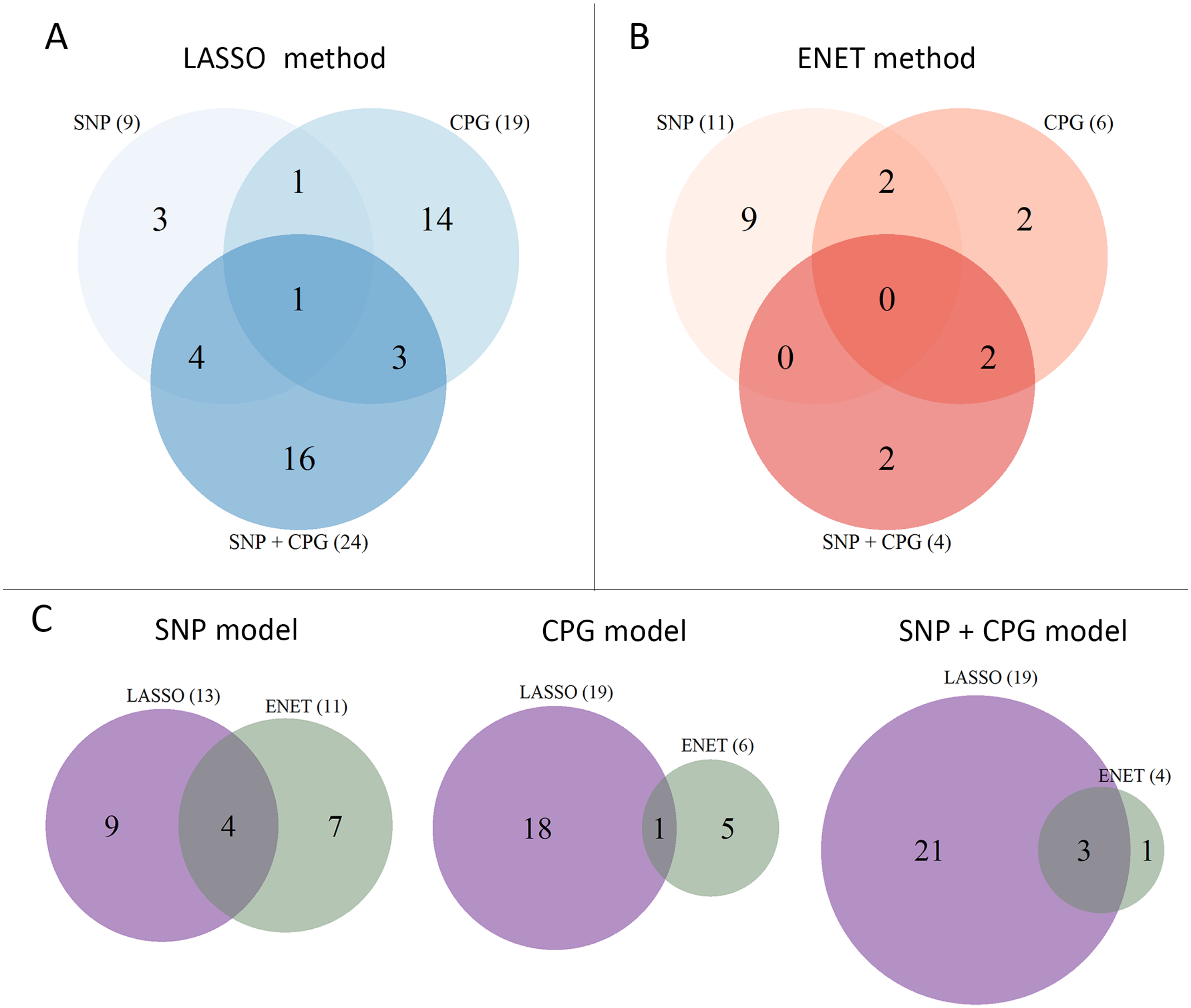

Fig 3. Venn diagrams showing the overlap between the significant genes compared by the two methods (LASSO and ENET) and models (SNPs, CpGs and Global). (A) Number of significant genes using the LASSO method for the three models (SNP, CPG, and Global); (B) number of significant genes using the ENET method for the three models (SNP, CPG and Global); and (C) number of significant genes per model comparing the two methods (LASSO and ENET).

doi:10.1371/journal.pgen.1005689.g003

parameter (Eq 5) used by LASSO is always equal to 1 while ENET uses $\alpha < 1$. This gives a smaller penalization and therefore more variables with $\beta \neq 0$ were foreseen using ENET; and (2) the fact that SNPs and CpGs may be correlated, mainly when they are closely positioned in the genome, leads LASSO to select one from the set of parameters that are highly correlated while ENET forms groups of nets with these variables. In our analysis, only 4/24 (SNP model), 1/25 (CpG model) and 3/28 (Global model) genes were shared by both methods. The genes detected only by LASSO showed large deviances and borderline p-values with ENET. Waldmann *et al* [35] reported that ENET usually detects more true and false positive associations. In our case, this may result in an increased probability of having significant associations by chance. In turn, this can lead to reduced power. On the other hand, ENET selected some genes

Table 3. Significant genes obtained by LASSO&Permuted based maxT algorithm for the three models (SNP, CPG, and Global) in the original dataset (EPICURO Study) and the replication dataset (TCGA).

	Original Data (EPICURO)												Validation Data (TCGA)				
	Gene	probeset	Chr	Start	end	Dev	p-value	SNPs (N)	CpGs (N)	Dev	p-value[1]	SNPs (N)	CpGs (N)	SNPs (overlap)	SNPs (rep)	CpGs (overlap)	CpGs (rep)
SNP model	*SERPINB3*	8023696	18	61322433	61329197	171.6	<0.01	29		0	1	0		3	0		
	SERPINB4	8023688	18	61304495	61311502	98.4	<0.01	15		0	1	0		2	0		
	CEACAM6	8029098	19	42259398	42276113	79.6	0.01	10		0	1	0		0	0		
	CLIC6	8068383	21	36041688	36090519	75.3	0.01	30		3.5E-08	0.9	1		14	0		
	CRTAC1	**7935535**	**10**	**99624758**	**99790585**	**66.2**	**0.03**	**18**		**2.4E+09**	**0.001**	**12**		**4**	**1 (LD)**		
	GSTT1	**8074980**	**22**	**24376141**	**24384284**	**40.4**	**0.07**	**16**		**8.3E+07**	**<0.001**	**34**		**4**	**1 (LD)**		
	PTN	8143144	7	136912092	137028546	67.0	0.08	9		0	1	0		1	0		
	SCNN1A	7960529	12	6456011	6486523	57.9	0.08	26		0	1	0		8	0		
	AIM2	**7921434**	**1**	**159032275**	**159046647**	**55.8**	**0.1**	**6**		**5.7E+05**	**0.03**	**1**		**2**	**0**		
CPG model	***CEACAM7***	**8037053**	**19**	**42177235**	**42192096**	**76.0**	**< 0.01**		**19**	**1.5E+07**	**< 0.001**		**2**			**17**	**0**
	PIGR	**7923929**	**1**	**207101869**	**207119811**	**75.8**	**< 0.01**		**21**	**6.4E+08**	**0.001**		**19**			**18**	**1**
	PLA2G2A	**7913216**	**1**	**20301925**	**20306932**	**71.4**	**0.01**		**10**	**5.2E+09**	**< 0.001**		**57**			**9**	**0**
	CP	**8091385**	**3**	**148890292**	**148939832**	**51.1**	**0.02**		**3**	**1.6E+09**	**< 0.001**		**24**			**1**	**0**
	HMGCS2	7919055	1	120290620	120311555	53.3	0.02		8	0	1		**0**			8	-
	KRT5	**7963427**	**12**	**52908361**	**52914243**	**58.2**	**0.02**		**25**	**3.6E+12**	**< 0.001**		**112**			**24**	**5**
	C15orf48	**7983478**	**15**	**45722763**	**45725645**	**49.9**	**0.02**		**7**	**1.5E+08**	**< 0.001**		**23**			**5**	**0**
	KRT13	**8015323**	**17**	**39657233**	**39661865**	**53.6**	**0.02**		**8**	**8.2E+11**	**< 0.001**		**5**			**6**	**0**
	IGJ	**8100827**	**4**	**71521259**	**71532348**	**58.4**	**0.03**		**2**	**4.2E+08**	**< 0.001**		**19**			**2**	**0**
	SCNN1A	**7960529**	**12**	**6456011**	**6486523**	**58.8**	**0.03**		**29**	**2.1E+09**	**< 0.001**		**12**			**27**	**0**
	S100A9	**7905571**	**1**	**153330330**	**153333502**	**53.7**	**0.04**		**11**	**5.0E+11**	**< 0.001**		**33**			**9**	**1**
	KRT20	**8015124**	**17**	**39032141**	**39041495**	**48.4**	**0.05**		**3**	**5.9E+09**	**< 0.001**		**45**			**3**	**0**
	CTSE	**7909164**	**1**	**206317459**	**206332103**	**60.7**	**0.06**		**12**	**3.4E+09**	**< 0.001**		**36**			**12**	**1**
	AIM2	**7921434**	**1**	**159032275**	**159046647**	**61.5**	**0.06**		**8**	**4.7E+07**	**0.002**		**27**			**4**	**0**
	OLFM4	**7969288**	**13**	**53602972**	**53626186**	**60.0**	**0.06**		**10**	**1.6E+10**	**< 0.001**		**47**			**9**	**6**
	MSMB	7927529	10	51549553	51562590	67.3	0.06		7	0	1		**0**			6	0
	FREM2	**7968678**	**13**	**39261173**	**39461265**	**46.0**	**0.08**		**2**	**4.4E+07**	**< 0.001**		**13**			**1**	**0**
	CLIC6	**8068383**	**21**	**36041688**	**36090519**	**45.1**	**0.09**		**4**	**1.2E+08**	**< 0.001**		**19**			**4**	**0**
	TNNT3	**7937749**	**11**	**1940799**	**1959935**	**44.9**	**0.09**		**26**	**5.2E+08**	**< 0.001**		**72**			**22**	**0**
Global model	***SERPINB3***	**7920285**	**18**	**61322433**	**61329197**	**162.7**	**<0.01**	**15**	**0**	**3.0E+09**	**<0.001**	**6**	**4**	**1**	**0**	**0**	**0**
	KRT20	**7905571**	**17**	**39032141**	**39041495**	**93.7**	**<0.01**	**19**	**7**	**5.7E+09**	**<0.001**	**8**	**38**	**0**	**0**	**0**	**0**
	PTN	**7935535**	**7**	**136912092**	**137028546**	**92.0**	**<0.01**	**12**	**0**	**2.6E+08**	**<0.001**	**0**	**1**	**0**	**0**	**0**	**0**
	SERPINB4	**7938758**	**18**	**61304495**	**61311502**	**68.6**	**0.03**	**4**	**0**	**7.9E+08**	**<0.001**	**27**	**11**	**0**	**0**	**0**	**0**
	SAA1	7962559	11	18287808	18291521	127.8	0.04	20	1	7.9E+08	0.6	0	1	5	1	0	0

(Continued)

Table 3. (*Continued*)

Original Data (EPICURO)												Validation Data (TCGA)				
Gene	probeset	Chr	Start	end	Dev	p-value	SNPs (N)	CpGs (N)	Dev	p-value[1]	SNPs (N)	CpGs (N)	SNPs (overlap)	SNPs (rep)	CpGs (overlap)	CpGs (rep)
S100A2	7957966	1	153533587	153538306	58.7	0.04	20	7	1.0E+11	<0.001	1	5	5	0	3	0
C15orf48	7964927	15	45722763	45725645	83.7	0.05	19	6	1.7E-07	<0.001	1	6	0	0	0	0
TSPAN8	7963817	12	71518877	71551779	67.2	0.05	8	1	9.9E+05	0.02	1	0	3	0	1	0
FREM2	7968678	13	39261173	39461265	70.2	0.06	14	2	2.9E+07	<0.001	3	10	3	0	1	0
CLIC6	7983478	21	36041688	36090519	75.3	0.07	25	2	1.4E+08	<0.001	21	15	0	1 (LD)	0	0
UBD	7995712	6	29523390	29527702	75.0	0.07	6	5	8.8E+08	<0.001	0	25	0	0	0	0
CAPNS2	7981724	16	55600584	55601592	54.9	0.07	8	1	5.8E+07	<0.001	10	12	0	0	0	0
MYBPC1	8023688	12	101988747	102079657	74.5	0.08	23	3	9.9E-08	1	0	1	2	0	2	0
TMEM45A	8037197	3	100211463	100296285	57.3	0.08	12	0	1.6E+08	0.001	11	19	0	1 (LD)	0	0
S100A9	8015124	1	153330330	153333502	52.5	0.08	6	4	4.9E+11	<0.001	15	24	0	1 (LD)	4	1
SLC38A4	8023696	12	47158544	47219780	51.7	0.08	15	1	1.6E+08	0.001	8	15	6	0	1	0
IGJ	8068383	4	71521259	71532348	59.0	0.09	3	2	3.3E+08	0.003	1	3	0	0	0	0
ARHGEF5	8081288	7	143883177	143892791	49.6	0.09	8	0	1.2E+07	<0.001	11	8	0	1 (LD)	0	0
CRTAC1	8100827	10	99624758	99790585	60.9	0.1	7	5	3.8E+09	<0.001	7	9	1	0	3	1
IGHD	8136981	14	106303102	106312014	59.4	0.1	7	1	-	-	-	-	-	-	-	-
CRH	8151092	8	67088612	67090846	56.7	0.1	3	0	9.4E+08	<0.001	7	10	0	0	0	0
TRIM31	8178330	6	30070674	30080867	47.1	0.1	23	4	5.8E+08	<0.001	0	43	0	0	0	0
CXCL17	8143144	19	42932696	42947136	46.8	0.1	3	5	7.4E+08	<0.001	8	11	0	0	0	0
GTSF1	8124650	12	54849737	54867386	46.7	0.1	2	1	2.1E+07	<0.001	18	46	2	0	1	1

[1] Bonferroni correction for the p-value were: 0.005 (SNP model), 0.003 (CPG model) and 0.002 (Global model); SNPs (N) and CpGs (N) are the number of SNPs and CpGs that were selected by LASSO per each gene expression probe in EPICURO data with the Illumina HumanHap 1M array and the Methylation 27k array; SNPs (overlap) and CpGs (overlap) are the number of SNPs and CpGs that were present in the TCGA data with the Genome wide 6.0 Affymetrix and the Methylation 450k array; and the SNPs (rep) and CpGs (rep) are the ones selected by LASSO in the TCGA data in common with the EPICURO data. The gene with "no p-value" is a gene that was not present in the RNASeqV2 in TCGA data.

doi:10.1371/journal.pgen.1005689.t003

that were not selected by LASSO, mainly due to the correlated structure of the parameters. An example of this is displayed in Fig 4, showing that *MMP7* has three correlation nets that probably are responsible for the gene selection with ENET and not with LASSO. These comparisons are shown in S4 Table.

Regarding the differences between the models, 13/25 and 6/20 significant genes in the CpG and 6/20 the SNP models, respectively, were not significant in the Global model. It is reported in the literature that 10% of SNPs are associated with gene expression and DNA methylation [36,37], hence DNA methylation may confound or modify the association between SNP and gene expression. Even though this is a potential explanation, discordances resulting from sample size cannot be discarded since the penalty function is selected by CV. However, k = 5 was used to apply the k-fold CV to decrease the problem of small sample size without increasing bias. In the reverse scenario, 16 genes were selected exclusively in the Global model. Some of

Table 4. Significant genes obtained by ENET&Permuted based maxT algorithm for the three models (SNP, CPG, and Global) in the original dataset (EPICURO Study) and the replication dataset (TCGA).

	Original Data (EPICURO)												Validation Data (TCGA)				
	Gene	probeset	Chr	Start	end	Dev	p-value	SNPs (N)	CpGs (N)	Dev	p-value[1]	SNPs (N)	CpGs (N)	SNPs (overlap)	SNPs (rep)	CpGs (overlap)	CpGs (rep)
SNP model	**ANXA10**	**8098246**	**4**	**169013707**	**169108891**	**137.0**	**0.01**	**17**		**1.4E+08**	**<0.001**	**13**		**7**	**1**		
	SERPINB3	8023696	18	61322433	61329197	171.6	0.02	30		1.4E+09	0.08	32		3	0		
	CEACAM6	8029098	19	42259398	42276113	108.4	0.03	28		1.4E+09	0.04	4		5	0		
	SERPINB4	8023688	18	61304495	61311502	105.2	0.04	31		1.1E+08	0.07	10		8	1 (LD)		
	GTSF1	7963817	12	54849737	54867386	109.6	0.05	19		1.6E+06	0.08	7		9	2 (LD)		
	IGF2	**7937772**	**11**	**2150348**	**2170833**	**101.6**	**0.05**	**56**		**3.9E+12**	**0.002**	**31**		**12**	**0**		
	IGLJ3	7981730	22	23247030	23247205	97.7	0.05	183		-	-	-		-	-		
	MMP7	**7951217**	**11**	**102391240**	**102401478**	**94.8**	**0.06**	**19**		**2.8E+08**	**0.004**	**10**		**6**	**1 (LD)**		
	PTN	8143144	7	136912092	137028546	97.2	0.07	24		0	1	0		10	0		
	MSMB	7927529	10	51549553	51562590	91.8	0.07	78		0	1	0		0	0		
	TCN1	7948444	11	59620281	59634041	88.9	0.07	122		0	1	0		0	0		
CPG model	*REN*	7923608	1	204123944	204135465	84.3	0.03		22	0	1		1			22	0
	IGF2	**7937772**	**11**	**2150348**	**2170833**	**92.1**	**0.04**		**15**	**8.1E+12**	**<0.001**		**609**			**12**	**7**
	NLRP2	**8031398**	**19**	**55476652**	**55512508**	**84.2**	**0.04**		**34**	**8.0E+08**	**< 0.001**		**10**			**28**	**2**
	CEACAM5	8029086	19	42212530	42234436	92.1	0.06		26	9.3E+08	0.009		1			23	0
	MSMB	7927529	10	51549553	51562590	78.9	0.06		9	6.2E+07	0.3		36			7	1
	CRABP2	**7921099**	**1**	**156669410**	**156675375**	**65.2**	**0.09**		**39**	**1.1E+10**	**<0.001**		**132**			**35**	**11**
Global model	***SERPINB3***	**7920285**	**18**	**61322433**	**61329197**	**171.3**	**0.01**	**27**	**1**	**5.3E+09**	**<0.001**	**37**	**15**	**0**	**0**	**1**	**1**
	MMP7	**7951217**	**11**	**102391240**	**102401478**	**99.4**	**0.08**	**62**	**18**	**2.3E+08**	**0.003**	**5**	**2**	**0**	**0**	**0**	**0**
	PTN	**8143144**	**7**	**136912092**	**137028546**	**102.5**	**0.09**	**20**	**0**	**6.1E+08**	**<0.001**	**16**	**15**	**0**	**0**	**0**	**0**
	IGHD	7981724	14	106303102	106312014	97.5	0.1	35	6	-	-	-	-	-	-	-	-

[1] Bonferroni correction for the p-values is: 0.008 (CPG model) and 0.01 (Global model); SNPs (N) and CpGs (N) are the number of SNPs and CpGs that were selected by ENET per each gene expression probe in EPICURO data with the Illumina HumanHap 1M array and the Methylation 27k array; SNPs (overlap) and CpGs (overlap) are the number of SNPs and CpGs that were present in the TCGA data with the Genome wide 6.0 Affymetrix and the Methylation 450k array and the SNPs (rep) and CpGs (rep) are the ones selected by ENET in the TCGA data in common with the EPICURO data. The gene with no p-value is a gene that was not present in the RNASeqV2 in TCGA data.

doi:10.1371/journal.pgen.1005689.t004

the genes identified had high deviances and borderline p-values, probably because the Global models increase the deviance due to the addition of more information when integrating data. For the nonsignificant genes, the explanation could be the existence of an interaction effect between SNPs and CpGs (S5 Table). This further supports the importance of integrating *omics* data to discover hidden information.

The validity of the strategy that we have developed, and of the results obtained, is supported by the fact that 75% (36/48) of the genes identified in the discovery phase were replicated using TCGA data by applying the same strategy. This represents 64% of all gene models found since some of the genes overlap between models and approaches. Also, the null results of the simulation study indicate that the significant associations found are unlikely to be due to chance.

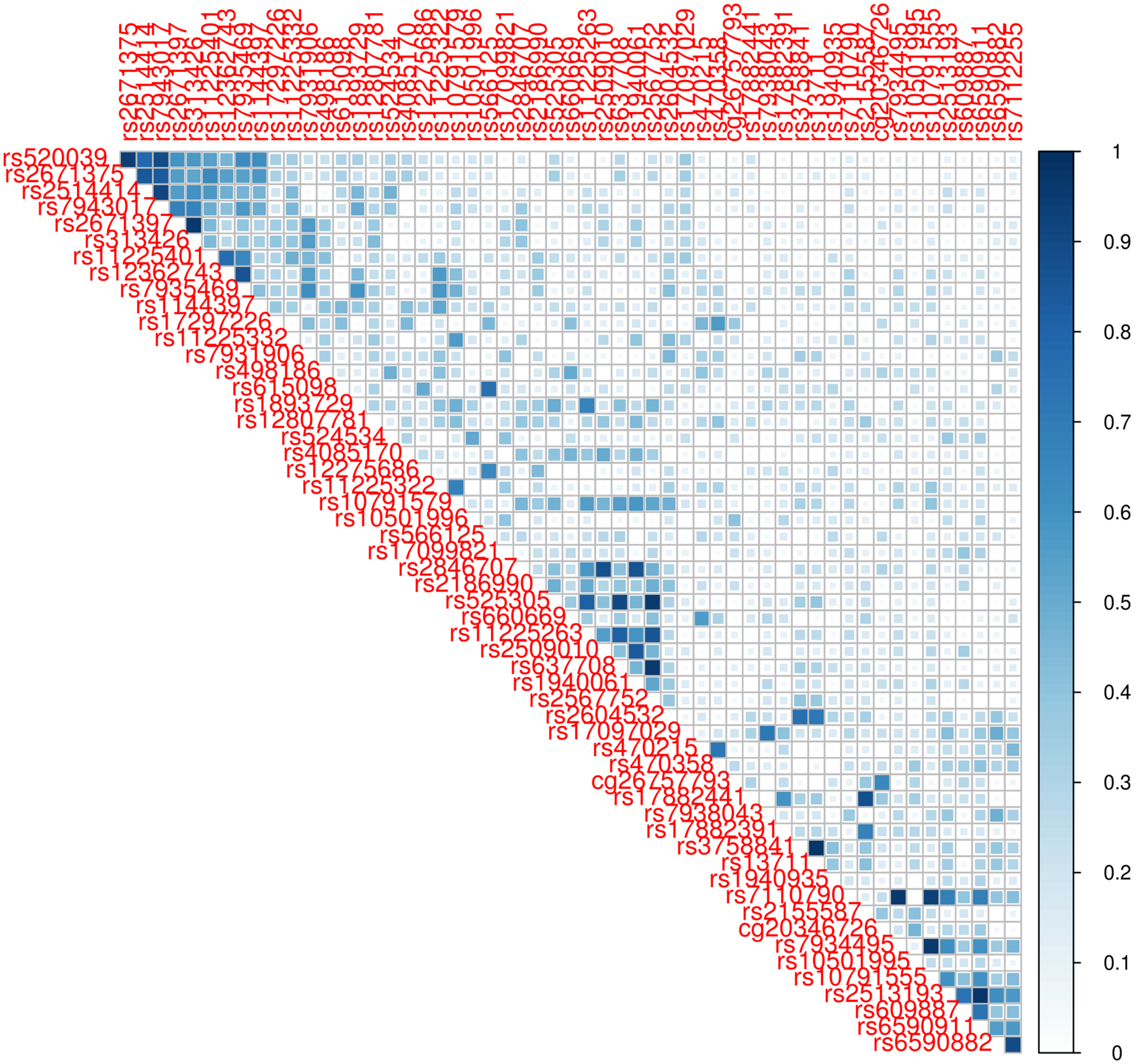

Fig 4. Example of a correlation plot for *MMP7* detected by the Global model using ENET but not using LASSO. The bar color represents the levels of correlation from 0 (no correlation) to 1 (perfect correlation) between SNPs and CpGs that were selected for the *MMP7* models. Three nets of correlated variables are the ones responsible that the gene is only selected by ENET and not by LASSO.

doi:10.1371/journal.pgen.1005689.g004

Importantly, several of the genes that emerged from our analyses have been previously shown to be important in bladder cancer biology, including *KRT20*, *IGF2*, *CTSE*, *ANXA10* and *CRH*. These genes have already been proposed for a panel of molecular markers to improve the diagnosis and follow-up of UBC as part of a 12-gene expression urine signature to identify patients suffering from UBC and predict tumor aggressiveness [38]. The five genes aforementioned were also replicated in the TCGA data. Furthermore, *KRT20*, *IGF2*, and *CTSE* have also been previously associated with UBC. *KRT20* is a highly specific marker of umbrella cells in normal urothelium and its expression is commonly altered in papillary non muscle-invasive UBC as well as in muscle-invasive UBC. It has been proposed that the correlation between *FGFR3* mutations with normal *KRT20* expression pattern may indicate that the mutation occurs earlier [39]. Loss of imprinting (LOI) is a common epigenetic event in cancer and a LOI of *IGF2* has been reported in UBC [40]. In our analysis, *IGF2* was detected in the SNP and CPG models suggesting that both type of factors may be involved in regulating the expression levels of this gene. *CTSE* expression was significantly associated with progression-free survival in pTa tumors in a study of gene expression profiles in UBC [41].

We also performed a gene enrichment analysis to assess whether the significant genes had related biological functions. The cluster with the highest ES was"Extracellular region, secreted, and signal peptide". Secreted proteins are known to play a crucial role in cell signaling and the cellular secretome has a major impact on multiple aspects of tumor cell biology (cell growth, migration, invasion, and angiogenesis) [42]. One cluster highly enriched in keratins points to the regulation of cell differentiation, known to be important in the molecular classification of UBC. In addition, some genes—including *S100A9* and *S100A2*—were grouped under the "EF hand and calcium ion binding" term. The *S100* family is composed of, at least, 24 members carrying the Ca^{2+} binding EF-hand motif. Expression of *S100* protein family members is regulated during inflammation and carcinogenesis and has been associated with poor prognosis in patients with UBC [43]. Other studies have reported an overexpression of *S100A9* in UBC tissue [44,45].

Limitations of this work are the small sample size of the discovery phase study, due to the lack of enough fresh tumor tissue from the same set of individuals, and the lack of a comparable and independent UBC patient series with the 3-*omics* data available to replicate our results. While the discovery EPICURO study recruited all patients with UBC, the TCGA project focused on muscle-invasive UBC. In addition, different highthroughput technologies/platforms were used in each of the studies. The SNP arrays genotyped different SNPs and, consequently, provided different genomic coverage. The TCGA used a DNA methylation array of 450k with much higher resolution than the 27k the one used in the EPICURO study. Finally, the use of different technologies to measure transcriptomics is a considerable limitation. In the EPICURO discovery phase, gene expression levels were measured with microarrays which provide relative values at probe set level, that is, for one gene different expression levels can be obtained from each mapped probe, while in the TCGA study gene expression was measured with RNA-seq which gives absolute gene expression values. These differences between data sets introduce a massive heterogeneity that makes the replication even more difficult. In spite of that, we replicated 75% of the identified genes (64% of the models) with TCGA data, providing strong support to the appropriateness of our approach and the relevance of the results obtained. Another potential limitation is the fact that tumor samples are heterogeneous regarding neoplastic cell content and stromal cell composition. Consequently, we checked the expression of all significant genes in a panel of UBC cell lines with available microarray expression data [46] and found that all but one (*IGJ*) are expressed in urothelial tumor cells, indicating that our analyses likely reflect genomic regulatory events in the tumor cells. It is, however, likely that relevant genomic interactions control gene expression not only in neoplastic cells but also in the stroma. Given the importance of the latter in tumor progression, further integrative *omics* studies using microdissected material will be highly informative.

One important strength of the approach used here is the lack of need to filter by LD in SNPs, or grouping CpGs within CpG islands, when dealing with a huge number of heterogeneous and correlated parameters delivered by different arrays. This emanates from the fact that LASSO and ENET can deal with highly correlated variables while performing variable selection. By performing data reduction/filtering before applying the statistical methods, there is a chance to filter out the functional SNPs and/or CpGs and thereby lose their association with gene expression. The adaptation of a strategy that performs a permutation and the maxT algorithm to assess p-values and to correct by MT, avoiding a double permutation and therefore reducing computational time, is also worthwhile emphasizing. In this regard, the permutation-based method considers the permutation of individuals within each gene, allowing to control for the possible dependence structure between genes. In addition, the MaxT algorithm is a permutationbased FWER controlling procedure which is adapted to the correlation structure found in the data and has been shown to be asymptotically optimal under dependence [47]

In summary, we demonstrate that the integration of multiple *omics* data types allows the identification of hidden mechanisms that were missed when analyzing single *omics* data types individually. There is an urgent need to develop statistical methods to fill the gap between the huge amount of data generated and the mechanistic understanding of complex diseases. Here, we present two penalized regression methods (LASSO and ENET) in combination with a permutation–based strategy (permutation-based MaxT method) to deal with common problems found in integrative analysis: heterogeneity between data types, number of individuals much smaller than the parameters to assess, multicollinearity, and sparseness to facilitate the interpretation of the results. This approach is flexible and easy to implement in different *omics* data and diseases as well as when considering interaction terms in the model.

We contribute to the field with a methodological development and with several significant and sound molecular associations conforming part of the genetic architecture of UBC. By using this cancer as an example, we conclude that modeling the intricacy of *omics* data variation with appropriate statistical strategies will certainly improve our knowledge of the mechanisms involved in complex diseases.

Data availability statement

Common genetic variation (GSE51641), DNA methylation (GSE71666), and gene expression (GSE71576) data for the discovery phase are available in GEO.

Supporting Information

S1 Excel. SNP-LASSO model. Information about SNPs associated with gene expression using LASSO with SNP model for the discovery and replication phase.
(XLSX)

S2 Excel. CPG-LASSO model. Information about CpGs associated with gene expression using LASSO with CPG model for the discovery and replication phase.
(XLSX)

S3 Excel. Global-LASSO model. Information about SNPs and CpGs associated with gene expression using LASSO with Global model for the discovery and replication phase.
(XLSX)

S4 Excel. SNP-ENET model. Information about SNPs associated with gene expression using ENET with SNP model for the discovery and replication phase.
(XLSX)

S5 Excel. CPG-ENET model. Information about CpGs associated with gene expression using ENET with CPG model for the discovery and replication phase.
(XLSX)

S6 Excel. Global-ENET model. Information about SNPs and CpGs associated with gene expression using ENET with Global model for the discovery and replication phase.
(XLSX)

S1 Fig. Deviance across the genome when applying LASSO for the SNP model for the simulated data. The number of genes simulated are 20,899 for 27 individuals using a multivariate normal distribution ($\mu = 8.4$, $\sigma^2 = 0.4$). No gene was significantly associated after the permutation-based MaxT algorithm.
(TIF)

S1 Table. IDs corresponding to the 27 samples from the EPICURO data used in this analysis.
(DOCX)

S2 Table. IDs corresponding to the 238 samples from the TCGA data used in this analysis.
(DOCX)

S3 Table. Functional Annotation Clustering from DAVID tool (Enrichment score $\geq$ 1.3).
(DOCX)

S4 Table. Comparison of the deviance, p-value and SNPs and/or CpGs detected by each model between LASSO and ENET methods.
(DOCX)

S5 Table. Comparison of genes selected by each model (SNP, CpG and Global model) using LASSO.
(DOCX)

Acknowledgments

We acknowledge the coordinators, field and administrative workers, technicians and patients of the pilot Spanish Bladder Cancer (SBC)/EPICURO Study.

Author Contributions

Conceived and designed the experiments: SP FXR KVS NM. Performed the experiments: SP FXR SJC. Analyzed the data: SP KVS NM. Contributed reagents/materials/analysis tools: FXR MK AC SJC NM. Wrote the paper: SP KVS NM FXR.

References

1. Greenawalt DM, Sieberts SK, Cornelis MC, Girman CJ, Zhong H, et al. (2012) Integrating genetic association, genetics of gene expression, and single nucleotide polymorphism set analysis to identify susceptibility Loci for type 2 diabetes mellitus. Am J Epidemiol 176: 423–430. doi:kws123 [pii] doi: 10.1093/aje/kws123 PMID: 22865700

2. Li Q, Seo JH, Stranger B, McKenna A, Pe'er I, et al. (2013) Integrative eQTLbased analyses reveal the biology of breast cancer risk loci. Cell 152: 633–641. doi:S0092-8674(12)01556-5 [pii] doi: 10.1016/j.cell.2012.12.034 PMID: 23374354

3. Serizawa RR, Ralfkiaer U, Steven K, Lam GW, Schmiedel S, et al. (2011) Integrated genetic and epigenetic analysis of bladder cancer reveals an additive diagnostic value of FGFR3 mutations and hypermethylation events. Int J Cancer 129: 78–87. doi: 10.1002/ijc.25651 PMID: 20824703

4. Hamid JS, Hu P, Roslin NM, Ling V, Greenwood CM, et al. (2009) Data integration in genetics and genomics: methods and challenges. Hum Genomics Proteomics 2009. doi: 10.4061/2009/869093

5. Chadeau-Hyam M, Campanella G, Jombart T, Bottolo L, Portengen L, et al. (2013) Deciphering the complex: methodological overview of statistical models to derive OMICS-based biomarkers. Env Mol Mutagen 54: 542–557. doi: 10.1002/em.21797

6. Kristensen VN, Lingjaerde OC, Russnes HG, Vollan HK, Frigessi A, et al. (2014) Principles and methods of integrative genomic analyses in cancer. Nat Rev Cancer 14: 299–313. doi:nrc3721 [pii] doi: 10.1038/nrc3721 PMID: 24759209

7. Ritchie MD, Holzinger ER, Li R, Pendergrass SA, Kim D (2015) Methods of integrating data to uncover genotype–phenotype interactions. Nat Rev Genet 16: 85–97. doi: 10.1038/nrg3868 PMID: 25582081

8. Shpak M, Hall AW, Goldberg MM, Derryberry DZ, Ni Y, et al. (2014) An eQTL analysis of the human glioblastoma multiforme genome. Genomics 103: 252–263. doi: 10.1016/j.ygeno.2014.02.005 PMID: 24607568

9. Bryois J, Buil A, Evans DM, Kemp JP, Montgomery SB, et al. (2014) Cis and trans effects of human genomic variants on gene expression. PLoS Genet 10: e1004461. doi: 10.1371/journal.pgen.1004461 PMID: 25010687

10. Drong AW, Nicholson G, Hedman AK, Meduri E, Grundberg E, et al. (2013) The presence of methylation quantitative trait loci indicates a direct genetic influence on the level of DNA methylation in adipose tissue. PLoS One 8: e55923. doi: 10.1371/journal.pone.0055923 PONE-D-12-31174 [pii]. PMID: 23431366

11. Heyn H, Sayols S, Moutinho C, Vidal E, Sanchez-Mut J V, et al. (2014) Linkage of DNA methylation quantitative trait Loci to human cancer risk. Cell Rep 7: 331–338. doi:S2211-1247(14)00194-6 [pii] doi: 10.1016/j.celrep.2014.03.016 PMID: 24703846

12. Pineda S, Gomez-Rubio P, Picornell A, Bessonov K, Márquez M, et al. (2015) Framework for the Integration of Genomics, Epigenomics and Transcriptomics in Complex Diseases. Hum Hered 79: 124–136. doi: 10.1159/000381184 PMID: 26201698

13. Parkhomenko E, Tritchler D, Beyene J (2009) Sparse canonical correlation analysis with application to genomic data integration. Stat Appl Genet Mol Biol 8: Article 1. doi: 10.2202/1544-6115.1406

14. De Tayrac M, Le S, Aubry M, Mosser J, Husson F (2009) Simultaneous analysis of distinct Omics data sets with integration of biological knowledge: Multiple Factor Analysis approach. BMC Genomics 10: 32. doi:1471-2164-10-32 [pii] doi: 10.1186/1471-2164-10-32 PMID: 19154582

15. Palermo G, Piraino P, Zucht HD (2009) Performance of PLS regression coefficients in selecting variables for each response of a multivariate PLS for omics-type data. Adv Appl Bioinform Chem 2: 57–70. PMID: 21918616

16. Tibshirani R (1996) Regression Shrinkage and Selection via the Lasso. J R Stat Soc Ser b 58: 267–288.

17. Hui Zou TH (2005) Regularization and variable selection via the Elastic Net. J R Stat Soc Ser B 67: 301–320.

18. Pineda S, Milne RL, Calle ML, Rothman N, López de Maturana E, et al. (2014) Genetic variation in the TP53 pathway and bladder cancer risk. a comprehensive analysis. PLoS One 9: e89952. doi: 10.1371/journal.pone.0089952 PMID: 24818791

19. Cho S, Kim K, Kim YJ, Lee J-K, Cho YS, et al. (2010) Joint identification of multiple genetic variants via elastic-net variable selection in a genome-wide association analysis. Ann Hum Genet 74: 416–428. doi: 10.1111/j.14691809.2010.00597.x PMID: 20642809

20. Zhou H, Sehl ME, Sinsheimer JS, Lange K (2010) Association screening of common and rare genetic variants by penalized regression. Bioinformatics 26: 2375–2382. doi: 10.1093/bioinformatics/btq448 PMID: 20693321

21. Mankoo PK, Shen R, Schultz N, Levine DA, Sander C (2011) Time to recurrence and survival in serous ovarian tumors predicted from integrated genomic profiles. PLoS One 6: e24709. doi: 10.1371/journal.pone.0024709 PMID: 22073136

22. Westfall Peter H., Young SS (1993) Resampling-based multiple testing: Examples and methods for p-value adjustment. Wiley-Interscience: New York. 360 pages p.

23. Hoerl AE, Kennard RW (1970) Ridge Regression: Biased Estimation for Nonorthogonal Problems. Technometrics 12: 55–67. doi: 10.1080/00401706.1970.10488634

24. Trevor Hastie; Rob Tibshirani; Jerome Friedman (2001) The Elements of Statistical Learning. Springer Series in Statistics.

25. Jerome Firedman; Trevor Hastie; Rob Tibshirani (2010) Regularization Paths for Generalized Linear Models via Coordinate Descent. J Stat Softw 33.

26. Ge Y, Dudoit S, Speed TP (2003) Resampling-based multiple testing for microarray data analysis. Test 12: 1–77. doi: 10.1007/BF02595811

27. Browning SR, Browning BL (2007) Rapid and accurate haplotype phasing and missing-data inference for whole-genome association studies by use of localized haplotype clustering. Am J Hum Genet 81: 1084–1097. doi: 10.1086/521987 PMID: 17924348

28. Zhu Y, Qiu P, Ji Y (2014) TCGA-assembler: open-source software for retrieving and processing TCGA data. Nat Methods 11: 599–600. doi: 10.1038/nmeth.2956 PMID: 24874569

29. Dennis G, Sherman BT, Hosack DA, Yang J, Gao W, et al. (2003) DAVID: Database for Annotation, Visualization, and Integrated Discovery. Genome Biol 4: P3. PMID: 12734009

30. Huang DW, Sherman BT, Lempicki RA (2009) Systematic and integrative analysis of large gene lists using DAVID bioinformatics resources. Nat Protoc 4: 44–57. doi: 10.1038/nprot.2008.211 PMID: 19131956

31. Benjamini Y, Hochberg Y (1995) Controlling the False Discovery Rate: A Practical and Powerful Approach to Multiple Testing. J R Stat Soc Ser b 57: 11.

32. Choi W, Czerniak B, Ochoa A, Su X, Siefker-Radtke A, et al. (2014) Intrinsic basal and luminal subtypes of muscle-invasive bladder cancer. Nat Rev Urol 11: 400–410. doi: 10.1038/nrurol.2014.129 PMID: 24960601

33. Knowles MA, Hurst CD (2014) Molecular biology of bladder cancer: new insights into pathogenesis and clinical diversity. Nat Rev Cancer 15: 25–41. doi: 10.1038/nrc3817

34. Leung D, Jung I, Rajagopal N, Schmitt A, Selvaraj S, et al. (2015) Integrative analysis of haplotype-resolved epigenomes across human tissues. Nature 518: 350–354. doi: 10.1038/nature14217 PMID: 25693566

35. Waldmann P, Mészáros G, Gredler B, Fuerst C, Sölkner J (2013) Evaluation of the lasso and the elastic net in genome-wide association studies. Front Genet 4: 270. doi: 10.3389/fgene.2013.00270 PMID: 24363662

36. Wagner JR, Busche S, Ge B, Kwan T, Pastinen T, et al. (2014) The relationship between DNA methylation, genetic and expression inter-individual variation in untransformed human fibroblasts. Genome Biol 15: R37. doi: 10.1186/gb-201415-2-r37 PMID: 24555846

37. Bell JT, Pai AA, Pickrell JK, Gaffney DJ, Pique-Regi R, et al. (2011) DNA methylation patterns associate with genetic and gene expression variation in HapMap cell lines. Genome Biol 12: R10. doi: 10.1186/gb-2011-12-1-r10 PMID: 21251332

38. Mengual L, Burset M, Ribal MJ, Ars E, Marín-Aguilera M, et al. (2010) Gene expression signature in urine for diagnosing and assessing aggressiveness of bladder urothelial carcinoma. Clin Cancer Res 16: 2624–2633. doi: 10.1158/1078-0432.CCR-09-3373 PMID: 20406841

39. Van Oers JMM, Wild PJ, Burger M, Denzinger S, Stoehr R, et al. (2007) FGFR3 mutations and a normal CK20 staining pattern define low-grade noninvasive urothelial bladder tumours. Eur Urol 52: 760–768. doi: 10.1016/j.eururo.2007.01.009 PMID: 17240035

40. Byun H-M, Wong H-L, Birnstein EA, Wolff EM, Liang G, et al. (2007) Examination of IGF2 and H19 loss of imprinting in bladder cancer. Cancer Res 67: 10753–10758. doi: 10.1158/0008-5472.CAN-07-0329 PMID: 18006818

41. Wild PJ, Herr A, Wissmann C, Stoehr R, Rosenthal A, et al. (2005) Gene expression profiling of progressive papillary noninvasive carcinomas of the urinary bladder. Clin Cancer Res 11: 4415–4429. doi: 10.1158/1078-0432.CCR05-0259 PMID: 15958626

42. Karagiannis GS, Pavlou MP, Diamandis EP (2010) Cancer secretomics reveal pathophysiological pathways in cancer molecular oncology. Mol Oncol 4: 496–510. doi: 10.1016/j.molonc.2010.09.001 PMID: 20934395

43. Yao R, Davidson DD, Lopez-Beltran A, MacLennan GT, Montironi R, et al. (2007) The S100 proteins for screening and prognostic grading of bladder cancer. Histol Histopathol 22: 1025–1032. PMID: 17523080

44. Dokun OY, Florl AR, Seifert H-H, Wolff I, Schulz WA (2008) Relationship of SNCG, S100A4, S100A9 and LCN2 gene expression and DNA methylation in bladder cancer. Int J Cancer 123: 2798–2807. doi: 10.1002/ijc.23893 PMID: 18803290

45. Minami S, Sato Y, Matsumoto T, Kageyama T, Kawashima Y, et al. (2010) Proteomic study of sera from patients with bladder cancer: usefulness of S100A8 and S100A9 proteins. Cancer Genomics Proteomics 7: 181–189. PMID: 20656984

46. Earl J, Rico D, Carrillo-de-Santa-Pau E, Rodríguez-Santiago B, Méndez-Pertuz M, et al. (2015) The UBC-40 Urothelial Bladder Cancer cell line index: a genomic resource for functional studies. BMC Genomics 16: 403. doi: 10.1186/s12864-015-1450-3 PMID: 25997541

47. Meinshausen N, Maathuis MH, Bühlmann P (2011) Asymptotic optimality of the Westfall–Young permutation procedure for multiple testing under dependence. Ann Stat 39: 3369–3391.